Myocardial Strain Analysis of Echocardiographic Sequences Using Non-Rigid Registration

MJ Ledesma-Carbayo[1], A Santos[1], J Kybic[2], P Mahía-Casado[3], MA García-Fernández[3], N Malpica[3], E Pérez-David[3], M Desco[3]

[1]Universidad Politécnica de Madrid, Spain
[2]Czech Technical University, Czech Republic
[3]Hopital General Universitario Gregorio Marañón, Madrid, Spain

Abstract

This paper proposes a new method to compute the 2D strain tensor from gray-scale 2D echocardiographic sequences and presents a clinical trial to test its applicability to regional analysis of the left ventricle.

Myocardial motion is computed using spatio-temporal non-rigid registration techniques on the whole sequence. The key feature of our method is the use of an analytical representation of the myocardial displacement field based on a semi-local parametric model of the deformation using Bsplines. The strain tensor is therefore obtained from the analytical expression of the spatial gradient of the displacement field. Robustness and speed are achieved by introducing a multiresolution-optimization strategy.

To test the clinical applicability of our method we applied the algorithm to the regional analysis of the left ventricle, and obtained significant differences between normal and pathological segments.

1. Introduction

Strain imaging introduced a new way to assess regional contractility. Its main advantage, in comparison with other myocardial parameters such as displacement and velocity, is that it describes the active motion of the myocardial muscle. In the presence of ischemic heart disease the affected segments have their contraction altered, however they may move because of the tethering of the neighbor segments.

Strain and strain rate have been calculated using ultrasound data derived from Doppler Velocity Imaging [1, 2]. However this measurement has a disadvantage: it only measures the deformation along the ultrasound beam direction and is very dependent on the signal to noise ratio of the Doppler data. Other approaches have explored the possibility of obtaining multidimensional strain using speckle tracking [3] and elastographic techniques [4, 5]. These methods relay on the processing of the RF signal to obtain the displacement of one or several consecutive lines of response, using correlation and phase shift techniques.

Another family of methods combine image features extraction and deformable and mechanical models. They have been intensively applied to extract strain information from Tagged MR imaging [6, 7], and recently from echocardiographic data [8]. The main drawback of these methods is that the strain parameters rely on a proper segmentation of the myocardial borders, a very difficult task on ultrasound data due to its poor signal to noise ratio.

Our work proposes a new method to compute the 2D strain tensor from gray-scale 2D echocardiographic sequences applying non-rigid registration techniques. Prior works using non-rigid registration techniques have been applied on Tagged-MR studies to compute cardiac motion [9, 10]. This work demonstrates the usefulness of these techniques on echocardiographic data performing a clinical trial to test its application for the regional analysis of the left ventricle.

2. Methods

2.1. Dense displacement field computation

Given an image sequence $f(t, \mathbf{x})$, the goal is to estimate a dense displacement field $\mathbf{g}(t, \mathbf{x})$ over the whole sequence. We choose to represent the movement with respect to the first frame of the sequence: a point at coordinate $\mathbf{x}$ in the first frame ($t = t_0$) will move to the location $\mathbf{g}(t, \mathbf{x})$ at time t. In other words, the warped sequence $f_w(t, \mathbf{x}) = f(t, \mathbf{g}(t, \mathbf{x}))$ should not move and be at all times as similar as possible to the reference frame. We express $\mathbf{g}(t, \mathbf{x})$ as a series of transformations between consecutive pairs of images $\mathbf{g}'_{\mathbf{t}}(\mathbf{x}_{t-1})$. Formulation is therefore defined as:

$$\mathbf{g}(t,\mathbf{x}) \equiv \mathbf{g_t}(\mathbf{x}) \quad \text{where} \quad t \in \{0,1,...,T-1\} \quad \text{and} \quad \mathbf{x} \equiv (x_1, x_2, ...x_n) \in \mathbf{I} \tag{1}$$

$$\mathbf{g}_t(\mathbf{x}) = \mathbf{g}'_t(\mathbf{x}_{t-1}) + \mathbf{g_{t-1}}(\mathbf{x}) \quad \text{where} \quad \mathbf{x}_{t-1} = \mathbf{g_{t-1}}(\mathbf{x}) \quad \text{and} \quad \mathbf{g}_0(\mathbf{x}) = \mathbf{x} \tag{2}$$

The transformation between consecutive frames $\mathbf{g}'_t$ is a linear combination of Bspline basis functions, located in a rectangular grid, as previously introduced in [11, 12].

$$\mathbf{g}'_t(\mathbf{x}) = \sum_{\mathbf{j}\in\mathbb{Z}^N} \mathbf{c_j} \beta_r \left(\mathbf{x}/h - \mathbf{j}\right) \tag{3}$$

The scale parameter h governs the space between the grid knots, the total number of parameters $\mathbf{c_j}$, and the smoothness of the solution.

The solution to this problem is then formulated as an optimization procedure that minimizes a criterion E to find the coefficients $\mathbf{c_j}$. E is defined as the sum of squared differences between consecutive frames. This optimization is solved using a gradient descent method. Speed and robustness is granted using a multiresolution approach.

The displacement field is also constrained using prior knowledge about the cardiac motion field. First, the motion at the reference frame $f(0,\mathbf{x})$ must be zero, and secondly we impose the cyclic behavior as $\mathbf{g}(0,\mathbf{x}) = \mathbf{g}(T,\mathbf{x})$. This last constraint is achieved performing the registration process in both directions (forward and backward), obtaining two estimations of the displacement at a given time t. The final estimation is computed as a weighted linear combination of both estimates.

$$\mathbf{g}_t(\mathbf{x}) = \omega_t \mathbf{g}^f_t(\mathbf{x}) + (1-\omega_t)\mathbf{g}^b_t(\mathbf{x}) \quad \text{with} \quad \omega_t = \frac{T-t}{T} \tag{4}$$

2.2. Myocardial strain tensor calculation

The movement of a non-rigid homogeneous body is usually composed of changes in shape, size and position [13]. It can be decomposed into a rigid and a non-rigid component. Given a non-rigid body B_0, with a particle at position $\mathbf{X}$, moved and deformed into body B_t, with a new position of the same particle at $\mathbf{x}$, we define the deformation gradient tensor as:

$$\mathbf{F} = \nabla_{\mathbf{X}}(\mathbf{x}); \quad F_{ij} = \frac{\partial x_i}{\partial X_j}; \quad F_{ij} = \frac{\partial u_i}{\partial X_j} + 1 \tag{5}$$

where $u = \mathbf{x} - \mathbf{X}$ is the displacement of the given particle.

$\mathbf{F}$ represents the body variations in shape, size and position. It can be decomposed in two matrices $\mathbf{F} = \mathbf{RU}$, where $\mathbf{R}$ is the rotation matrix y $\mathbf{U}$ is the right stretch tensor. This decomposition is quite complex therefore the Cauchy-Green tensor is also defined as $\mathbf{C} = \mathbf{F}^T\mathbf{F} = U^2$. This formulation allows the definition of the Green-Lagrange strain tensor as:

$$\mathbf{E} = \frac{1}{2}(\mathbf{C} - \mathbf{I}) = \frac{1}{2}(\mathbf{F}^T\mathbf{F} - \mathbf{I}) \tag{6}$$

where $\mathbf{E} = 0$ when no deformation exists.

Given the dense displacement field $\mathbf{g}(t,\mathbf{x})$ introduced in the previous section and taking into account equations (5), we can calculate $\mathbf{F}$ in the bidimensional case as:

$$\mathbf{F} = \nabla_{\mathbf{x}}\,\mathbf{g} + I = \begin{bmatrix} \frac{\partial g_1}{\partial x_1} & \frac{\partial g_1}{\partial x_2} \\ \frac{\partial g_2}{\partial x_1} & \frac{\partial g_2}{\partial x_2} \end{bmatrix} + I \tag{7}$$

The Green-Lagrange strain tensor $\mathbf{E}$ is then easily computed from equation (6). Components $\frac{\partial g_i}{\partial x_j}$ can be calculated analytically in the case of our deformation model (3) as it is defined through Bspline functions. The deformation tensor is then projected onto the directions of interest to calculate the deformation in a determined direction.

2.3. Application to the regional analysis of the left ventricle

To test the procedure on clinical studies we acquired data with a Siemens Acuson Sequoia from 6 healthy volunteers and 6 patients with known coronary artery disease. We analyzed the basal and mid segments for the inferior (2C view) and septal walls (4C view). Regional function of each segment was qualitatively assessed by an expert, classifying them in three groups (Normal, Hypokinetic and Akinetic), yielding a total of 46 segments (24 healthy, 9 hypokinetic and 13 akinetic). The parameters studied were the peak systolic longitudinal (E_{long}) and radial (E_{rad}) strains. We compared the three groups through a one-way analysis of variance (ANOVA) with Sheffé post-hoc correction for multiple comparisons.

Non rigid registration was performed for every sequence using quadratic Bsplines to represent the deformation and a scale parameter h in pixels equivalent to 1 cm. These optimum parameters were obtained through validation on synthetic sequences as described in [14]. The dense displacement field and strain tensor were calculated following the methodology described in subsections 2.1 and 2.2.

In every sequence we defined the longitudinal axis of the left ventricle from the middle point of the mitral valve to the apex. The unitary vector of the longitudinal axis serves as a reference to define the unitary vectors of the

main directions of interest. $\mathbf{v}_{\text{long}}$, unitary vector of the axis, defined the longitudinal direction, and $\mathbf{v}_{\text{rad}}$, unitary vector perpendicular to the axis, the radial direction. The unitary vectors were then used to project the strain tensor obtaining the strain in both directions as:

$$E_{\text{rad}} = \mathbf{v}_{\text{rad}}^T \, \mathbf{E} \, \mathbf{v}_{\text{rad}} \quad E_{\text{long}} = \mathbf{v}_{\text{long}}^T \, \mathbf{E} \, \mathbf{v}_{\text{long}} \tag{8}$$

3. Results

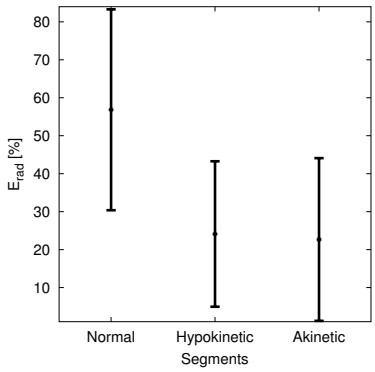

(a)

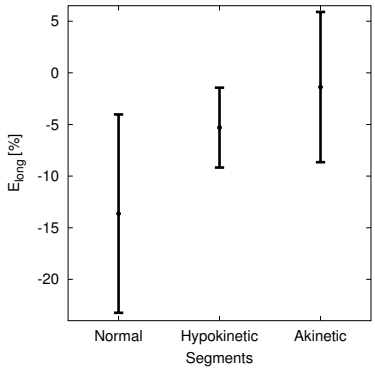

(b)

Figure 1. Mean and standard deviation of E_{rad} (a) and E_{long} (b) for the three groups. Normal segments $N = 24$. Hypokinetic segments $N = 9$. Akintetic segments $N = 13$

E_{long} ($M \pm SD$) showed significant differences ($p < 0.05$) between normal ($E_{\text{long}} = -15.2 \pm 6.0\%$) and akinetic segments ($E_{\text{long}} = -0.5 \pm 7.6\%$), between normal and hypokinetic ones ($E_{\text{long}} = -8.5 \pm 6.8\%$), and between akinetic and hypokinetic. E_{rad} showed significant differences ($p < 0.05$) between normal ($E_{\text{rad}} = 55.8 \pm 21.8\%$) and akinetic segments ($E_{\text{rad}} = 13.9 \pm 10.7\%$), and between normal and hypokinetic ones ($E_{\text{rad}} = 20.8 \pm 8.7\%$). No significant difference was found between akinetic and hypokinetic segments with E_{rad}.

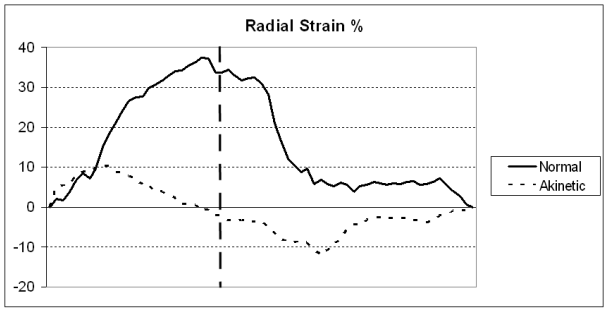

(a)

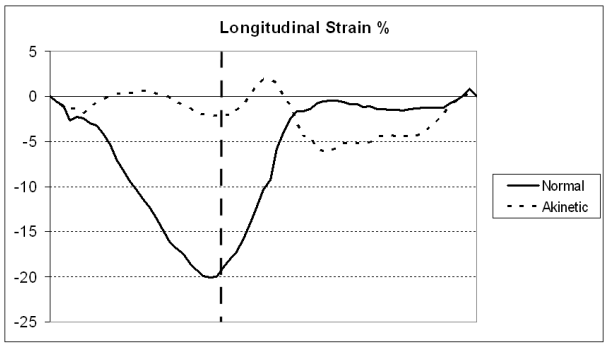

(b)

Figure 2. (a) Radial and (b) longitudinal strain time curves of the medial septal segment for a normal and an akinetic segment from two different subjects. End of systole is marked with a vertical dashed line.

Figure 2 shows an example of the radial and longitudinal strain time curves in the medial septal segment. This data were obtained from two different subjects: a healthy subject and a patient with an anterior infarct that affected the medial and apical septal segments. The different behavior of the normal and akinetic strains is clearly noticeable.

4. Discussion and conclusions

Results on myocardial strain estimation reveal the potential of this technique to provide a new method of asssement of myocardial strain from echocardiographic data, overcoming the limitations of the Doppler techniques. The strain values obtained are consistent with those previously published and obtained with Doppler derived techniques [15, 16], and Tagged MR data[17, 18].

This work shows the feasibility of computing systolic radial and longitudinal strains from gray scale echocardiographic sequences. Results show significant differences between normal and pathological segments, thereby illustrating the clinical applicability of the method proposed.

Acknowledgements

This work was supported in part by the grant *Red Temática IM3* from the Spanish Health Ministry (G03/185). The authors would like to acknowledge Jose María Goicolea for useful discussions on continuum mechanics theory.

References

[1] D'hooge J, Heimdal A, Jamal F, Kukuslki T, Bijnens B, Rademakers F, Hatle L, Suetens P, Sutherland G. Regional strain and strain rate measurements by cardiac ultrasound: Principles, implementation and limitations. Eur J Echocardiography 2000;1:154–170.

[2] Santos A, Ledesma-Carbayo M, Malpica N, Desco M, Antoranz J, Marcos-Alberca P, García-Fernández M. Accuracy of heart strain rate calculation derived from doppler tissue velocity data. In Insana MF, Shug K (eds.), Medical Imaging 2001, volume 4325. SPIE, 2001; 546–556.

[3] Kaluzynski K, Chen X, Emelianov S, Skovoroda A, O'Donnell M. Strain rate imaging using two-dimensional speckle tracking. IEEE Trans Ultrason Ferroelec Freq Contr 2001;48(4):1111–1123.

[4] Konofagou E, Ophir J. A new elastographic method for estimation and imaging of lateral displacements, lateral strains, corrected axial strains and poisson's ratios in tissues. Ultrasound Med Biol 1998;24(8):1183–99.

[5] D'hooge J, Konofagou E, Jamal F, Heimdal A, Barrios L, Bijnens B, Thoen J, Van de Werf F, Sutherland G, Suetens P. Two-dimensional ultrasonic strain rate measurement of the human heart in vivo. IEEE Trans Ultrason Ferroelec Freq Contr 2002;49(2):281–286.

[6] Shi P, Sinusas AJ, Constable RT, Ritman E, Duncan JS. Point-tracked quantitative analysis of left ventricular motion from 3D image sequences. IEEE Trans Med Imag 2000;19(1):36–50.

[7] Declerck J, Feldmar J, Ayache N. Defininion of a 4D continuous planispheric transformation for the tracking and the analysis of left-ventricle motion. Med Image Anal 1998; 2(2):197–213.

[8] Papademetris X, Sinusas AJ, Donald DP, Duncan JS. Estimation of 3D left ventricular deformation from echocardiography. Med Image Anal 2001;5(1):17–28.

[9] Ozturk C, McVeigh ER. Four-dimensional B-spline based motion analysis of tagged MR images: introduction and in vivo validation. Phys Med Biol 2000;45(6):1683–1702.

[10] Chandrashekara R, Mohiaddin RH, Rueckert D. Analysis of myocardial motion in tagged MR images using nonrigid image registration. In Proc. SPIE Medical Imaging 2002: Image Processing. San Diego, CA, USA, February 2002; 1168–1179.

[11] Kybic J, Unser M. Fast parametric elastic image registration. IEEE Trans Image Process 2003;12(11):1427–1442.

[12] Ledesma-Carbayo M, Kybic J, Desco M, Santos A, Unser M. Cardiac motion analysis from ultrasound sequences using non-rigid registration. In Niessen W, Viergever M (eds.), MICCAI 2001, Lecture Notes in Computer Science, volume 2208. Springer, October 2001; 889–896.

[13] Spencer AJM. Continuum mechanics. Longman Group Limited, London, 1980.

[14] Ledesma-Carbayo MJ. Cardiac Motion Detection using Elastic Registration. Ph.D. thesis, Universidad Politécnica de Madrid, Spain, 2003.

[15] Kukulski T, Jamal F, Herbots L, D'hooge J, Bijnens B, Hatle L, De Scheerder I, Sutherland G. Identification of acutely ischemic myocardium using ultrasonic strain measurements. a clinical study in patients undergoing coronary angioplasty. J Am Coll Cardiol 2003;41(5):810–819.

[16] Kowalski M, Kukulski T, Jamal F, D'hooge J, Weidemann F, Rademakers F, Bijnens B, Hatle L, Sutherland G. Can natural strain and strain rate quantify regional myocardial deformation? A study in healthy subjects. Ultrasound Med Biol 2001;27(8):1087–1097.

[17] Herbots L, Maes F, D'hooge J, Claus P, Dymarkowski S, Mertens P, Mortelmans L, Bijnens B, Bogaert J, Rademakers FE, Sutherland GR. Quantifying myocardial deformation throughout the cardiac cycle: a comparison of ultrasound strain rate, grey-scale m-mode and magnetic resonance imaging. Ultrasound Med Biol 2004;30(5):591–598.

[18] Moore C, Lugo-Olivieri C, McVeigh E, Zerhouni E. Three-dimensional systolic strain patterns in the normal human left ventricle: characterization with tagged MR imaging. Radiology 2000;214(2):453–466.

Address for correspondence:

María J. Ledesma-Carbayo
Dept. Ingeniería Electrónica
ETSI Telecomunicación
Ciudad Universitaria sn
E-28040 Madrid (Spain)
mledesma@die.upm.es